Kinetics and Mechanism of the Complex Formation of Ethylenediaminetetraacetatoferrate(III) with Sulfur(IV) Oxides in Aqueous Solution

Margareta Dellert-Ritter and Rudi van Eldik *

Institute for Inorganic Chemistry, University of Witten/Herdecke, Stockumer Strasse 10, 5810 Witten, Germany

A detailed kinetic study has been undertaken of the complex formation of $[Fe(edta)]^-$ (edta = ethylenediaminetetraacetate) with sulfite as a function of pH, [Fe(edta)] and [sulfite], during which stopped-flow and temperature-jump techniques were employed. The complex formation kinetics is controlled by the equilibria $[Fe(edta)(H_2O)]^- \rightleftharpoons [Fe(edta)(OH)]^{2-} + H^+$ and $2[Fe(edta)(OH)]^{2-} \rightleftharpoons [(edta)Fe\text{-}O\text{-}Fe(edta)]^{4-} + H_2O$, in which the aqua complex is extremely labile and the hydroxo and oxo complexes are substitution inert. The rate constant for the formation of $[Fe(edta)(SO_3)]^-$ from $[Fe(edta)(H_2O)]^-$ and SO_3^{2-} was found to be 4×10 dm^3 mol^{-1} s^{-1} at 25 °C and 0.5 mol dm^{-3} ionic strength. A limiting rate constant of 2×10^5 s^{-1} was reached at high $[SO_3^{2-}]$ under which conditions the dissociation of the co-ordinated water molecule becomes the rate-determining step. This observation is in agreement with the known solvent-exchange rate constant for $[Fe(edta)(H_2O)]^-$ and supports the operation of a limiting D mechanism. Both kinetic techniques revealed evidence for the participation of a slow, sulfite-independent reaction step, which could be related to the rate-determining dissociation of $[(edta)Fe\text{-}O\text{-}Fe(edta)]^{4-}$ at higher complex concentrations. The results are discussed with reference to the available literature data.

There is continuing interest in the kinetic behaviour of ethylenediaminetetraacetate (edta) and related complexes of $Fe^{II,III}$, especially in terms of their reactions with O_2, O_2^- and H_2O_2.[1–6] These reactions have gained importance in biochemical processes since they can be used for sequence-specific recognition and cleavage of DNA.[7–9] However, little is known about the fundamental substitution behaviour of $Fe^{II,III}$(edta) complexes, mainly because these reactions are extremely fast and difficult to follow owing to their small spectral changes.

In the present study we have selected sulfite as the substituting ligand and have studied its reactions with $[Fe^{III}(edta)]^-$ over a wide pH range. This reaction is accompanied by significant spectral changes, which enables the employment of stopped-flow and temperature-jump techniques to follow the substitution process. Our interest in this particular system originates from a series of studies on the iron(III)-catalysed autoxidation of sulfur(IV) oxides in aqueous solution,[10–14] suggested to play a significant role in atmospheric oxidation processes, *viz.* the formation of acid rain.[15–17] Our studies revealed rather complicated mechanistic behaviour, partly due to the high reactivity of the iron(III) centre and the large number of available co-ordination sites. These factors complicated the identification of intermediate iron(III)–sulfur(IV) complexes, which are produced prior to the redox reactions and play a key role in the catalytic cycle. In an effort to gain more insight into the mechanism of the catalysed autoxidation process, we decided to introduce a chelating ligand on the iron(III) centre in order to simplify the system. In the case of the $[Fe(edta)]^-$ complex, the majority of the co-ordination sites are blocked by the edta ligand such that only limited substitution by sulfite can occur. In addition, the sulfito complexes produced are significantly more redox stable than in the case of Fe^{III}, which enables a closer identification.

In this paper we report a detailed kinetic study of the substitution of $[Fe(edta)]^-$ by sulfite in aqueous solution. The redox behaviour of the sulfito complexes produced in the absence and presence of oxygen are reported in the following paper.[18]

Experimental

Aqueous solutions of $[Fe(edta)]^-$ were prepared from either a mixture of the components $Fe(ClO_4)_3 \cdot 9H_2O$ (Ventron) and $Na_2(H_2edta) \cdot 2H_2O$ (Merck) or $Na_4(edta) \cdot 2H_2O$ (Fluka), or directly from the solid Na[Fe(edta)] (Fluka). Chemicals of analytical reagent grade and deionized water were used throughout this study. The salt $NaClO_4 \cdot H_2O$ (Merck) was used to adjust the ionic strength of the test solutions, whereas NaOH and $HClO_4$ were used to adjust the pH. The latter was measured on a Metrohm instrument equipped with a glass electrode of which the reference compartment was filled with 3 mol dm^{-3} NaCl to prevent precipitation of $KClO_4$ when KCl was used instead of NaCl.

The UV/VIS spectra were recorded on Perkin-Elmer Lambda 5, Hitachi U 3200 and Shimadzu UV 250 spectrophotometers, IR spectra of aqueous solutions with an ATR cell using a Nicolet 5 SX FT-IR instrument. Rate measurements were performed on a Durrum D110 stopped-flow instrument, coupled to a data-acquisition system,[19] and on a Messanlagen (Göttingen) temperature-jump instrument. Both these instruments were thermostatted to ± 0.1 °C. Rate constants were in general measured on the stopped-flow instrument under pseudo-first-order conditions and the corresponding first-order plots were linear for at least 2 to 3 half-lives of the reaction. The reported rate constants were calculated with a standard least-squares program and are mean values from at least five kinetic runs.

Results and Discussion

Properties of $[Fe(edta)]^-$.—An important aspect of this study concerns the nature of the co-ordination geometry and structure of the $[Fe^{III}(edta)]^-$ species in aqueous solution. Various groups have investigated this system and we will only summarize the most important findings.[20] In general, edta acts as a sexidentate ligand and forms very stable complexes with Fe^{III} and related metal ions.[21] X-Ray structure analyses of various $[Fe(edta)]^-$ crystalline states[22–25] have clearly

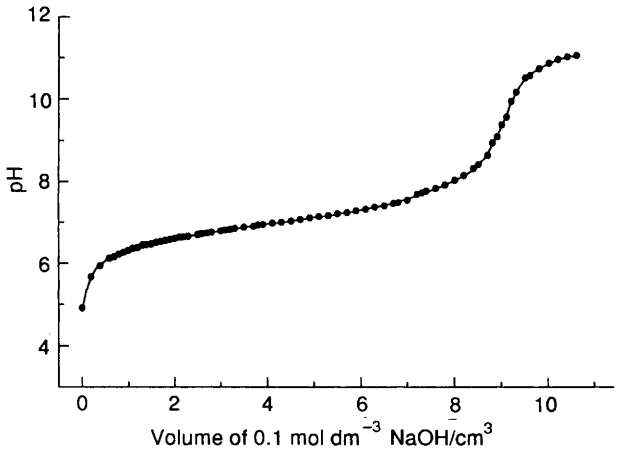

Fig. 1 pH Titration of 50 cm^3 2 × 10^{-2} mol dm^{-3} Na[Fe(edta)] with 0.1 mol dm^{-3} NaOH at 25 °C and I = 0.5 mol dm^{-3}

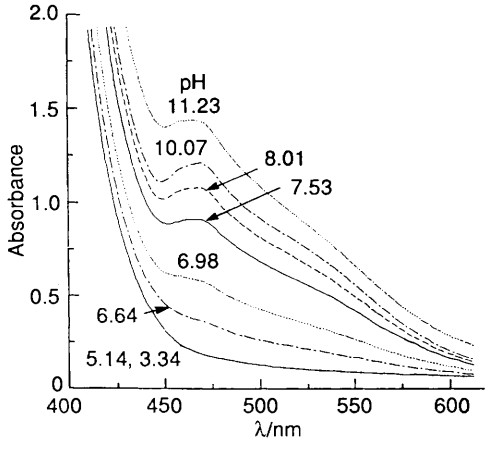

Fig. 2 UV/VIS spectra of 2 × 10^{-2} mol dm^{-3} [Fe(edta)]$^-$ as a function of pH at 25 °C and I = 0.3 mol dm^{-3}

shown these to be sexidentate seven-co-ordinate complexes with an approximate pentagonal-bipyramidal structure. Further studies[26-32] have demonstrated that this structure is retained in solution, *i.e.* a sexidentate seven-co-ordinate species involving a co-ordinated water molecule, *viz.* [Fe(edta)(H_2O)]$^-$. It was also suggested that, on protonation in an acidic medium, ring opening occurs to produce a quinquedentate seven-co-ordinate diaqua complex, [Fe(Hedta)(H_2O)$_2$], or a quinquedentate six-co-ordinate aqua complex, [Fe(Hedta)(H_2O)], of which the free carboxylate arm is protonated.[23,33-35] By way of comparison, X-ray structures have confirmed that [Cr(Hedta)(H_2O)] and K[Cr(edta)]·2H_2O are both six-co-ordinate with edta acting as quinque- and sexi-dentate, respectively.[36,37] In solution it was shown that these species exist in equilibrium,[38,39] although the participation of a sexidentate seven-co-ordinate complex [Cr(edta)(H_2O)]$^-$ cannot be ruled out.[20]

It follows from the above discussion that aqueous solutions of [Fe(edta)]$^-$ should exhibit characteristic acid–base equilibria. This property has resulted in conflicting reports in the literature due to the uncertain number of co-ordinated water molecules on the iron(III) centre that can undergo deprotonation. In earlier studies it was reported that [Fe(edta)]$^-$ exhibits two deprotonation steps with acid-dissociation constants (pK_a) of 7.49 and 9.41, respectively.[40,41] In other work and in this study, evidence for only one deprotonation step could be found in the range pH 4–11, which is assigned to reaction (1). The value of pK_1 varied between 7.4 and 7.7 depending on the experimental conditions employed, especially the ionic strength of the medium.[30,31,42] Evidence for the formation of [Fe(edta)(OH)$_2$]$^{3-}$ comes from NMR data,[30] which indicate a pK_a value of 10.2 for the [Fe(edta)(OH)]$^{2-}$ species. The value of K_1 can be determined accurately from a potentiometric or spectrophotometric titration of either 1:1 mixtures of $Fe(ClO_4)_3$ and $Na_2(H_2edta)$ or $Na_4(edta)$, or of Na[Fe(edta)]. A typical example of such a titration curve is given in Fig. 1, from which it follows that there

$$[Fe(edta)(H_2O)]^- \overset{K_1}{\rightleftharpoons} [Fe(edta)(OH)]^{2-} + H^+ \quad (1)$$

is no evidence for a second deprotonation step at pH ≤ 11. The pK_1 values measured in this study as a function of complex concentration and ionic strength revealed a steady decrease from 7.8 to 7.2 on increasing the ionic strength from 1 × 10^{-3} to 0.5 mol dm^{-3}.

Detailed potentiometric studies of the hydrolysis equilibria[41,42] have revealed evidence for the formation of a dimeric species as indicated in equation (2), where each unit of the dimer takes a quinquedentate six-co-ordinate geometry both in the solid state and in aqueous solution.[32] Combination of equations (1) and (2) results in the overall equilibrium (3), for

$$2[Fe(edta)(OH)]^{2-} \overset{K_2}{\rightleftharpoons} [(edta)Fe\text{–}O\text{–}Fe(edta)]^{4-} + H_2O \quad (2)$$

$$2[Fe(edta)(H_2O)]^- \overset{K_3}{\rightleftharpoons} [(edta)Fe\text{–}O\text{–}Fe(edta)]^{4-} + 2H^+ + H_2O \quad (3)$$

which $K_3 = K_1^2K_2$. Typical values reported in the literature[42] at 25 °C are pK_1 = 7.58, log K_2 = 2.95 and pK_3 = 12.21.

Additional information on the equilibria in solution comes from UV/VIS spectra recorded as a function of pH and [Fe(edta)$^-$]. At a relatively low [Fe(edta)$^-$] of 2 × 10^{-4} mol dm^{-3} an absorbance maximum occurs at 255 nm (ε = 9000 ± 200 dm^3 mol^{-1} cm^{-1}) for pH 3.7 ± 0.1. On increasing the pH gradually the absorbance maximum shifts to 242 nm (ε = 8000 ± 200 dm^3 mol^{-1} cm^{-1}) for pH 10.0 ± 0.5 with an isosbestic point at 242 nm. These observations are in good agreement with those reported in the literature,[31,41] *viz.* maxima at 256 (9300) and 240 nm (ε = 8800 dm^3 mol^{-1} cm^{-1}) at low and high pH, respectively. These spectral changes are assigned to the deprotonation of [Fe(edta)(H_2O)]$^-$ to produce [Fe(edta)(OH)]$^{2-}$ during the increase in pH from 3 to 10. Significantly different spectral changes are observed at higher complex concentrations and longer wavelength. Spectra recorded for a 5 × 10^{-3} mol dm^{-3} solution as a function of pH exhibit the formation of a broad band at 470 nm, which is seen even more clearly for a 2 × 10^{-2} mol dm^{-3} solution as shown in Fig. 2. The formation of the band at 470 nm is further accompanied by the formation of a broad shoulder at *ca.* 540 nm. These spectral changes are ascribed to the formation of [Fe(edta)(OH)]$^{2-}$ followed by the dimerization reaction (2) at these relatively high complex concentrations. The overall equilibrium (3) is shifted towards the left at low pH and low complex concentrations. These observations are in good agreement with similar ones reported in the literature.[31,41-45] Various indications of the concentration level of the dimer are given in the literature ranging from 11% in a 10^{-4} mol dm^{-3} complex solution at pH > 8[31,42] to 38% in a 3 × 10^{-3} mol dm^{-3} solution at pH 9.[41] It was suggested that the bridged species is produced when the aqua and hydroxo complexes react at the pK_1 value.[44,45] The formation of a di-μ-hydroxo bridged complex followed by the loss of a water molecule was also suggested.[41-45]

Analysis of the spectral data recorded in this study (typical examples are shown in Fig. 2) on the basis that the dimeric species has a molar absorption coefficient of 115 dm^3 mol^{-1} cm^{-1} at 540 nm[41] indicated that a maximum concentration of

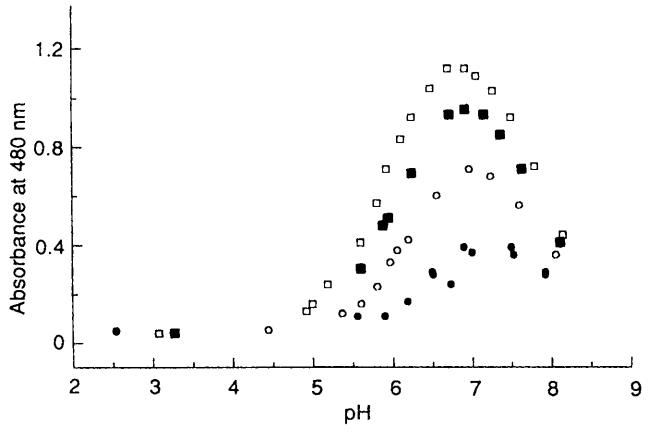

Fig. 3 Absorbance at 480 nm as a function of pH for various $[S^{IV}]_T$. Experimental conditions: $[Fe(edta)^-] = 5 \times 10^{-3}$ mol dm^{-3}; $[S^{IV}]_T = 5 \times 10^{-2}$ (●), 0.10 (○), 0.15 (■) or 0.20 mol dm^{-3} (□)

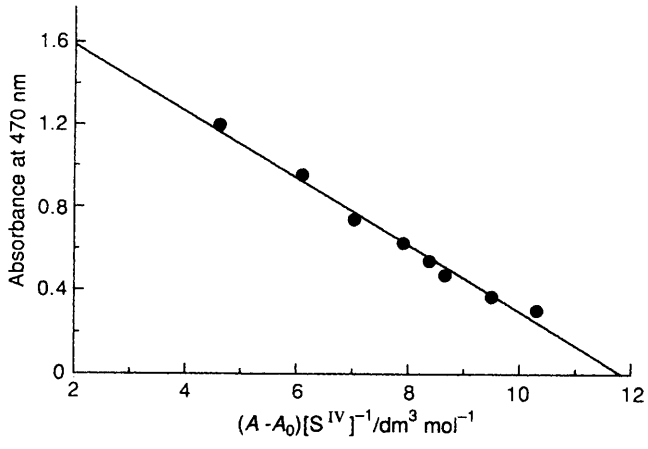

Fig. 4 Plot of absorbance *versus* $(A - A_0)/[S^{IV}]$ according to equation (8) for the reaction $[Fe(edta)(H_2O)]^- + SO_3^{2-} \rightleftharpoons [Fe(edta)(SO_3)]^{3-} + H_2O$. Experimental conditions: $[Fe(edta)^-] = 5 \times 10^{-3}$ mol dm^{-3}, pH 7.2; 25 °C, $I = 0.5$ mol dm^{-3}

the dimer is reached at pH $\geqslant pK_1$. This concentration amounts to *ca.* 20% of the total Fe^{III} for a 5×10^{-3} mol dm^{-3} solution and to *ca.* 50% for a 2×10^{-2} mol dm^{-3} solution. No evidence for the formation of dimeric species was found at $[Fe^{III}]_T = 2 \times 10^{-4}$ mol dm^{-3}.

Fourier-transform techniques using an ATR cell were employed in an effort to obtain additional structural information on the $[Fe(edta)]^-$ complex in acidic solution. Measurements were performed in water and D_2O as solvents. Good resolved spectra could be obtained for 0.25 mol dm^{-3} solutions of $[Fe(edta)]^-$, which are in good agreement with that reported for the solid complex.[46] The antisymmetric vibrations of the CO_2^- group shows a shift from 1620 cm^{-1} at pH 7 to lower wavenumbers on decreasing the pH and results in two peaks at 1614 and 1607 cm^{-1} at pH ≈ 1. This is interpreted in terms of dechelation of the ligand at lower pH[23,33-35] since the more ionic the nature of the group the lower is the wavenumber.[46] These results further support the suggestion that all the carboxylate groups on the edta ligand are co-ordinated to the iron centre at pH $\geqslant 5$, *i.e.* we are dealing with a seven-co-ordinate aqua complex under such conditions.

Formation of $[Fe(edta)(SO_3)]^{3-}$.—With the information reported in the previous section on the nature of the $[Fe(edta)]^-$ species in aqueous solution it is now possible to study the reactions with sulfite. In this respect we must consider the set of equilibria (4)–(6) for which selected values for the equilibrium

$$H_2O + SO_2 \overset{K_4}{\rightleftharpoons} HSO_3^- + H^+ \quad (4)$$

$$HSO_3^- \overset{K_5}{\rightleftharpoons} SO_3^{2-} + H^+ \quad (5)$$

$$2HSO_3^- \overset{K_6}{\rightleftharpoons} S_2O_5^{2-} + H_2O \quad (6)$$

constants at 25 °C are[11] $K_4 = 1.26 \times 10^{-2}$ mol dm^{-3}, $K_5 = 5.01 \times 10^{-7}$ mol dm^{-3} and $K_6 = 8.8 \times 10^{-2}$ dm^3 mol^{-1}. It follows that the main sulfur(IV) oxide species in solution can be SO_2, HSO_3^- or SO_3^{2-} depending on the pH of the solution. A disulfite $S_2O_5^{2-}$ species is formed at high concentrations of HSO_3^-, but the magnitude of K_6 is such that $S_2O_5^{2-}$ will exist as ⩾99% HSO_3^- at $[S_2O_5^{2-}]_T \leqslant 0.05$ mol dm^{-3}. The $[Fe(edta)]^-$–sulfite mixtures at pH 4.2–7.2, *i.e.* where mainly HSO_3^- and SO_3^{2-} are present in solution, respectively, produced yellow to orange solutions accompanied by significant absorbance increases at >450 nm due to complex formation. On further increasing the pH to 8.7, decomposition of the sulfito complex occurs which is accompanied by the formation of substitution-inert hydroxo and dimeric species. This trend can be seen more clearly from a series of absorbance measurements as a function of pH at various sulfite concentrations as shown in Fig. 3, and is in good agreement with the reported pK_1 value for the co-ordinated water molecule. The absorbance at 470 nm increases with increasing sulfite concentration and reaches a limiting value at high sulfite concentrations. In terms of the complex formation equilibrium (7), the equilibrium constant K_7

$$[Fe(edta)(H_2O)]^- + SO_3^{2-} \overset{K_7}{\rightleftharpoons} [Fe(edta)(SO_3)]^{3-} + H_2O \quad (7)$$

$$K_7 = (A - A_0)/(A_\infty - A)[SO_3^{2-}]$$

or

$$A = -\frac{A - A_0}{K_7[SO_3^{2-}]} + A_\infty \quad (8)$$

can be estimated from the absorbance data when plotted according to equation (8) as indicated in Fig. 4, where A_0, A and A_∞ are the absorbances at 470 nm following the addition of no, some and a large excess of sulfite, respectively. The data in Fig. 4 result in $K_7 = 6.2 \pm 0.3$ dm^3 mol^{-1}, and $A_\infty = 1.91 \pm 0.06$ ($\varepsilon = 380$ dm^3 mol^{-1} cm^{-1}) at pH 7.2. Similar measurements at higher pH resulted in lower values of K_7 (for instance 5.3 dm^3 mol^{-1} at pH 7.5) due to the interference from substitution-inert $[Fe(edta)(OH)]^{2-}$ species under such conditions.

The complex formation with sulfite was also studied using the described Fourier-transform IR technique. For this purpose spectra of 0.25 mol dm^{-3} $[Fe(edta)]^-$ in D_2O were recorded as a function of added Na_2SO_3. Three new bands at 1213, 1093 and 923 cm^{-1} appeared during the addition of sulfite, the first and last of which also occur for solutions of Na_2SO_3 in D_2O. It follows that the band at 1093 cm^{-1} is due to the formation of the sulfito complex and it is ascribed to the S–O stretching frequency of co-ordinated sulfite. It has been reported in the literature[47] that such a band is characteristic for the formation of a S-bonded sulfito complex since O-bonded sulfito complexes exhibit stretching bands below 960 cm^{-1}.

In a series of experiments the stability of the $[Fe(edta)(SO_3)]^{3-}$ complex was investigated by pH titration with acid and base. The titration of a 1:1 mixture of $[Fe(edta)]^-$ and Na_2SO_3 (both 1×10^{-2} mol dm^{-3}) with base resulted in a very similar titration curve as shown in Fig. 1, with a pK value of 7.3. This indicates that a 1:1 mixture is not sufficient to co-ordinate the Fe(edta). In the presence of an excess of sulfite the titration with acid shows a pK at 6.4 which is in agreement with the

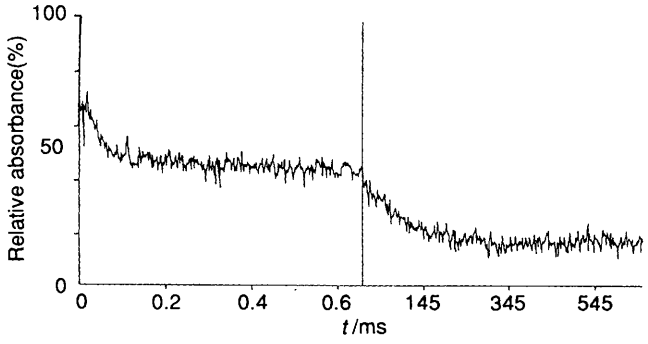

Fig. 5 Temperature-jump signals observed for the process $[Fe(edta)(H_2O)]^- + SO_3^{2-} \rightleftharpoons [Fe(edta)(SO_3)]^{3-} + H_2O$. Experimental conditions: $[Fe(edta)^-] = 1 \times 10^{-3}$ mol dm^{-3}, $[S^{IV}]_T = 0.04$ mol dm^{-3}, pH 8.13, $\lambda = 340$ nm, 25 °C ($\Delta T \approx 3$ °C)

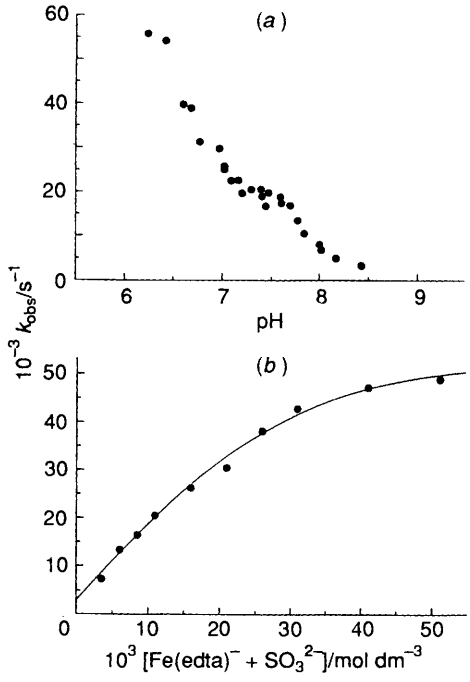

Fig. 6 Rate constant k_{obs} as a function of (*a*) pH ($[S^{IV}]_T = 1 \times 10^{-2}$ mol dm^{-3}) and (*b*) sulfite concentration (pH 7.3) for the formation of $[Fe(edta)(SO_3)]^{3-}$ (temperature-jump data). Experimental conditions: $[Fe(edta)^-] = 1 \times 10^{-3}$ mol dm^{-3}, $I = 0.3$ mol dm^{-3}, 25 °C, $\lambda = 340$ nm

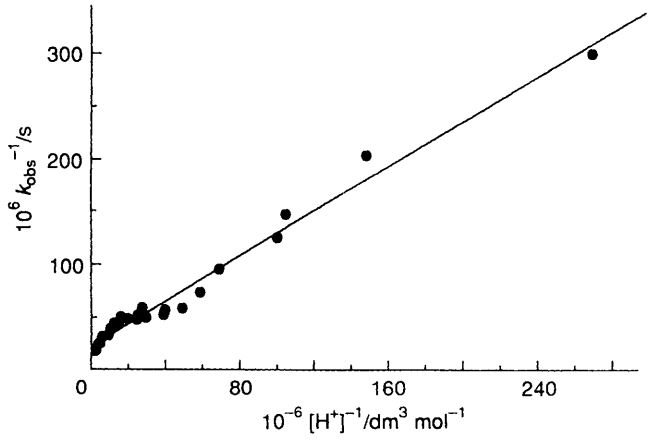

Fig. 7 Plot of k_{obs}^{-1} *versus* $[H^+]^{-1}$ for the data in Fig. 6(*a*) according to equation (11)

protonation of SO_3^{2-} as shown in reaction (5). These processes were also followed spectrophotometrically and similar conclusions were reached.

Kinetic Measurements.—The observed spectral changes associated with the complex formation reaction (7) can be employed to study the kinetics of this reaction using temperature-jump and stopped-flow techniques. Preliminary experiments on equilibrated solutions of $[Fe(edta)]^-$–SO_3^{2-} mixtures, exhibited depending on the selected experimental conditions, two temperature-jump relaxations, a typical example of which is shown in Fig. 5. The kinetic data for the slow relaxation agree very well with those obtained from the stopped-flow experiments (see further Discussion). The fast relaxation exhibits characteristic pH and $[S^{IV}]_T$ dependences (see Fig. 6). Notwithstanding the relatively large experimental error limits (up to 10%) involved in these measurements, which are mainly due to the weak intensity of the observed relaxation signals, the observed trends in the rate data are significant. The pH dependence of the fast reaction can be interpreted in terms of the reaction scheme outlined in (9), for which the rate equation is (10) when an excess of sulfite is employed.

$$\begin{array}{ccc} [Fe(edta)(H_2O)]^- & \overset{K_1}{\rightleftharpoons} & [Fe(edta)(OH)]^{2-} + H^+ \\ +SO_3^{2-} & & +SO_3^{2-} \\ k_a \uparrow\downarrow k_{-a} & & k_b \uparrow\downarrow k_{-b} \\ [Fe(edta)(SO_3)]^{3-} & + H_2O/OH^- & \end{array} \quad (9)$$

$$k_{obs} = \left(\frac{k_a[H^+] + k_bK_1}{[H^+] + K_1}\right)[SO_3^{2-}] + (k_{-a} + k_{-b}) \quad (10)$$

The significantly more labile aqua complex accounts for the increase in k_{obs} with decreasing pH, and for the disappearance of the relaxation at pH >8.5 [Fig. 6(*a*)]. It follows that $k_a \gg k_b$ and $(k_{-a} + k_{-b})$ is small, such that equation (10) can be simplifed as shown in (11). At constant $[SO_3^{2-}]$, equation (11) predicts a

$$k_{obs} = k_a[H^+][SO_3^{2-}]/([H^+] + K_1) \quad (11)$$

linear relationship between k_{obs}^{-1} and $[H^+]^{-1}$. This is indeed the case for the data in Fig. 6(*a*) as shown in Fig. 7, from which it follows that $k_a = 4.3 \times 10^6$ dm^3 mol^{-1} s^{-1} and $pK_1 = 7.3$. The latter value is in good agreement with that determined potentiometrically in this study.

The sulfite concentration dependence of the fast relaxation [Fig. 6(*b*)] demonstrates that k_{obs} is a linear function of $[Fe(edta)^- + SO_3^{2-}]$ (expressed in this way since sulfite is not in a large excess under all conditions) at low sulfite concentration, *i.e.* under the conditions where the pH dependence was investigated. The intercept of this plot is rather small and represents $(k_{-a} + k_{-b})$ according to equation (10). Furthermore, Fig. 6(*b*) indicates that a limiting value for k_{obs} is reached at high sulfite concentration. The fact that the substitution reaction becomes independent of $[SO_3^{2-}]$ may be an indication for the operation of a limiting D mechanism, in which case the dissociation of a water molecule becomes the rate-determining step under such conditions. The suggested mechanism based on the observed pH dependence, namely that the aqua complex is the main reactive species, is outlined in equation (12). For this

$$\begin{array}{ccc} [Fe(edta)(H_2O)]^- & \overset{k_s}{\underset{k_{-s}}{\rightleftharpoons}} & [Fe(edta)]^- + H_2O \\ & & +SO_3^{2-} \\ & & k_{-q} \uparrow\downarrow k_q \\ & & [Fe(edta)(SO_3)]^{3-} \end{array} \quad (12)$$

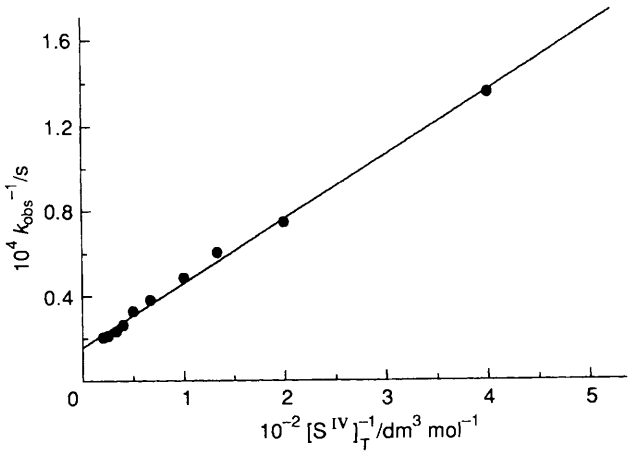

Fig. 8 Plot of k_{obs}^{-1} *versus* $[S^{IV}]_T^{-1}$ for the data in Fig. 6(*b*) according to equation (13)

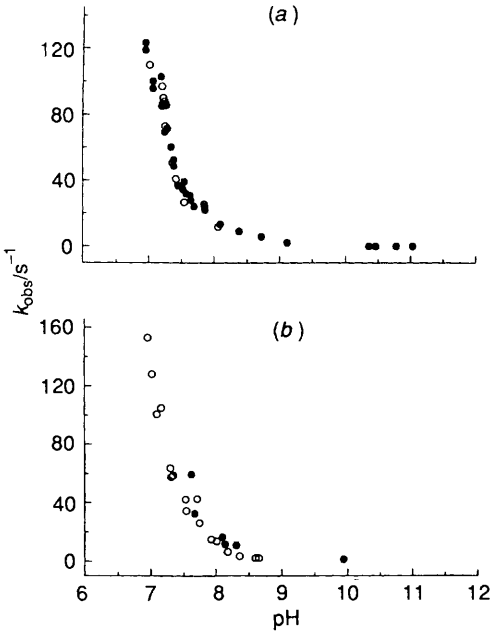

Fig. 9 Rate constants k_{obs} as a function of pH for (*a*) the apparent formation of $[Fe(edta)(SO_3)]^{3-}$ and (*b*) the equilibration of the $[Fe(edta)]^-$ system according to equation (3). Experimental conditions: (*a*) λ = 360 nm, 25 °C, I = 0.5 mol dm^{-3}, $[Fe(edta)^-]$ = 1 × 10^{-3} (SF) or 5 × 10^{-3} mol dm^{-3} (TJ), $[S^{IV}]_T$ = 1 × 10^{-2} (SF) or 5 × 10^{-2} mol dm^{-3} (TJ); (*b*) I = 0.3 mol dm^{-3}, 25 °C ($\Delta T \approx 3$ °C for TJ data), $[Fe(edta)^-]$ = 1 × 10^{-3} (TJ) or 5 × 10^{-3} mol dm^{-3} (SF), λ = 340 (TJ) or 470 nm (SF). ●, Stopped-flow (SF) measurements; ○, temperature-jump (TJ) measurements

mechanism the appropriate rate expression is (13), for which it

$$k_{obs} = k_8k_9[SO_3^{2-}]/(k_{-8} + k_9[SO_3^{2-}]) + k_{-9} \quad (13)$$

can be assumed that k_{-9} is rather small, *i.e.* the intercept in Fig. 6(*b*). Under these conditions the limiting rate constant at high $[SO_3^{2-}]$ should be k_8 and a plot of k_{obs}^{-1} *versus* $[SO_3^{2-}]^{-1}$ should be linear with intercept k_8^{-1} and slope k_{-8}/k_8k_9. The corresponding plot in Fig. 8 demonstrates the validity of the above simplification and results in a k_8 value of 6.3 × 10^4 s^{-1} and a k_{-8}/k_9 value of 0.02 mol dm^{-3} at pH 7.3. The latter ratio demonstrates the higher nucleophilicity of sulfite compared to water especially when k_{-8} is expressed as a second-order rate constant since then the ratio has a value of 3.5 × 10^{-4}. Results similar to those reported in Fig. 6(*b*) were also found for a series of experiments at pH 8.1.[48] An alternative mechanism to account for the non-linear dependence of k_{obs} on $[SO_3^{2-}]$ could be an interchange process involving formation of the ion pair $[Fe(edta)(H_2O)]^-\cdot SO_3^{2-}$. However, the double reciprocal plot then results in an ion-pair formation constant of 50 dm^3 mol^{-1}, which is unrealistic for ion-pair formation between similarly charged ions.

The above reported value of k_8 at pH 7.3, *viz.* 6.3 × 10^4 s^{-1}, should when extrapolated to lower pH, *i.e.* where $[Fe(edta)(H_2O)]^-$ is the only species in solution, correspond to the water-exchange rate constant for this complex. With the aid of the pH dependence reported in Fig. 6(*a*), k_8 can be extrapolated to *ca.* 1.8 × 10^5 s^{-1} at low pH, which is close to the literature value of 8 × 10^5 s^{-1} obtained from NMR relaxation experiments.[28] The operation of a dissociative mechanism as outlined in equation (12) can be ascribed to the labilization effect of the edta chelate, which results in a much higher solvent-exchange rate constant for $[Fe(edta)(H_2O)]^-$ than for $[Fe(H_2O)_6]^{3+}$.[28] Furthermore, the dissociative behaviour of the aqua complex is in line with the seven-co-ordinate structure of this complex in solution, which cannot undergo substitution in any other way. Similar results were recently reported for water exchange of the aqua(*o*-phenylenediamine-*N*,*N*,*N*′,*N*′-tetraacetato)ferrate(III) complex, which is also a seven-co-ordinate species.[49] The positive volume of activation was interpreted in terms of a dissociative-interchange mechanism.

At this point it is important to note an apparent discrepancy in the data. From the intercept and initial slope of Fig. 6(*b*) it is possible to calculate the overall equilibrium constant for the formation of $[Fe(edta)(SO_3)]^{3-}$, *viz.* $k_8k_9/k_{-8}k_{-9}$ according to the mechanism in equation (12). This value turns out to be *ca.* 260 dm^3 mol^{-1}, which is significantly larger than that determined spectrophotometrically, *viz.* $K_7 \approx 6$ dm^3 mol^{-1}. A likely explanation is that the latter value was determined in an overall thermodynamic way and may include for instance a pre-equilibrium between six- and seven-co-ordinated $[Fe(edta)(H_2O)]^-$ species[50] (see earlier Discussion) or a post-equilibrium between such species for the $[Fe(edta)(SO_3)]^{3-}$ complex. Whatever the nature of this equilibrium, its formation constant must be *ca.* 4 × 10^{-2} in order to resolve this apparent discrepancy.

Preliminary stopped-flow kinetic measurements indicated that kinetic traces can only be obtained at pH ≥6.9 and $[Fe(edta)^-] \geq 1 \times 10^{-3}$ dm^3 mol^{-1} with sulfite in at least a ten-fold excess to ensure pseudo-first-order behaviour. At lower pH and complex concentration no significant kinetic signal could be recorded on the stopped-flow time-scale (dead time of 2–4 ms). Some preliminary experiments were performed in the presence of 0.1 mol dm^{-3} tris(hydroxymethyl)aminomethane (Tris) buffer, and indicated a direct reaction between $[Fe(edta)]^-$ and the buffer. No buffer was therefore employed in all subsequent work, and where possible the buffer properties of the sulfite system were employed. The observed first-order rate constants strongly depend on pH in the range 7–11, with an exponential decrease in k_{obs} with increasing pH as demonstrated in Fig. 9(*a*). These results are in exact agreement with the data found for the second slow relaxation in the temperature-jump experiments, for which the data are also included in Fig. 9(*a*). If the observed kinetic traces represent a complex formation reaction, which could in principle account for the observed pH dependence, it is reasonable to expect that k_{obs} will depend on $[S^{IV}]_T$. A series of experiments at different pH (see Table 1) demonstrated that the observed reaction (stopped-flow and second temperature-jump relaxation) is independent of $[S^{IV}]_T$ under all conditions. The slight decrease observed in k_{obs} with increasing $[S^{IV}]_T$ at some pH is ascribed to a slight change in pH along the series of experiments, since no buffer could be employed.

In order to elucidate the nature of the slow kinetic step observed in both the temperature-jump and stopped-flow experiments a series of experiments were performed on solutions of $[Fe(edta)]^-$ in the absence of added sulfite. These exhibited a clear temperature-jump relaxation in the range

Table 1 Rate constant k_{obs} as a function of $[S^{IV}]_T$ for the slower reaction observed for the $[Fe(edta)]^-$–SO_3^{2-} system[a]

λ[b]/nm	[Tris buffer]/mol dm^{-3}	I/mol dm^{-3}	pH[c]	$[S^{IV}]_T$/mol dm^{-3}	k_{obs}[d]/s^{-1}	Method
340	0.1	0.3	7.20	1.0×10^{-3}	91.3	TJ
				5.0×10^{-3}	91.5	
				1.0×10^{-2}	101	
				1.5×10^{-2}	110	
				2.0×10^{-2}	86.6	
				2.5×10^{-2}	85.4	
				3.0×10^{-2}	87.9	
				3.5×10^{-2}	90.2	
360	0.1	0.5	8.25	1.0×10^{-2}	23.0	SF
				2.5×10^{-2}	23.3	
				5.0×10^{-2}	22.3	
				7.5×10^{-2}	20.2	
				0.10	19.2	
				0.125	19.0	
			9.0	1.0×10^{-2}	7.16	
				2.5×10^{-2}	6.11	
				5.0×10^{-2}	7.69	
				7.5×10^{-2}	6.78	
				0.10	6.71	
				0.125	6.45	
360	—	0.5	7.50	1.0×10^{-2}	25.8	SF
			7.56	2.0×10^{-2}	24.9	
			7.62	3.0×10^{-2}	24.2	
			7.71	4.0×10^{-2}	23.6	
			7.74	5.0×10^{-2}	22.8	
			8.74	1.0×10^{-2}	2.26	
			8.79	2.0×10^{-2}	1.74	
			8.70	3.0×10^{-2}	1.80	
			8.71	4.0×10^{-2}	1.51	
			8.60	5.0×10^{-2}	1.55	
			9.47	1.0×10^{-2}	0.72	
			9.37	2.0×10^{-2}	0.84	
			9.49	3.0×10^{-2}	0.65	
			9.41	4.0×10^{-2}	0.58	
			9.44	5.0×10^{-2}	0.55	
			10.5	5.0×10^{-3}	0.050	
			10.5	1.0×10^{-2}	0.050	
			10.5	1.5×10^{-2}	0.050	
			10.4	2.0×10^{-2}	0.050	
			10.4	5.0×10^{-2}	0.050	
			11.0	5.0×10^{-3}	0.018	
			11.0	1.0×10^{-2}	0.019	
			10.9	1.5×10^{-2}	0.018	
			10.9	2.0×10^{-2}	0.018	
			10.9	5.0×10^{-2}	0.017	

[a] $[Fe(edta)^-] = 1.0 \times 10^{-3}$ mol dm^{-3}, 25.0 °C. [b] Wavelength at which kinetic measurements were performed. [c] Only one pH value is quoted for the experiments in which Tris buffer was used since the pH was identical for the different solutions. [d] Mean value of at least four kinetic experiments with an average standard deviation of 10% for the temperature-jump (TJ) and 5% for the stopped-flow (SF) measurements.

pH 7–9, for which the results are summarized in Fig. 9(*b*). Surprisingly, the rate data for this relaxation in the absence of added sulfite exactly coincide with those observed for the slow step in the presence of sulfite. This observation indicates that we are dealing with a kinetic step in the $[Fe(edta)]^-$ system itself, which is also the rate-determining step during the slow reaction with sulfite. The most likely possibility involves the dimeric complex produced in reaction (3), which on dissociation forms the labile aqua complex that can rapidly undergo substitution by sulfite. This means that the rate data recorded for this complex must represent those for the equilibration process in (3). A few blank stopped-flow experiments were performed at 470 nm (*i.e.* where the bridged complex exhibits a maximum, see Fig. 2), in which solutions of $[Fe(edta)]^-$ were mixed with the solvent at the same ionic strength and pH. Such experiments indeed resulted in absorbance decreases [equilibrium (3) is shifted to the left] and kinetic data in excellent agreement with those obtained using temperature-jump techniques [see Fig. 9(*b*)]. In addition, a few experiments at significantly lower complex concentration (2×10^{-4} mol dm^{-3}) indicated no kinetic signals, in agreement with the absence of the bridged species under such conditions.[41–44]

It follows that the slow reaction observed must be due to the equilibration process outlined in (3) and a subsequent fast reaction of the aqua complex with sulfite as shown in (14).[44] The contribution of this step will only be significant at higher complex concentrations and at pH values close to the pK_1 value of the aqua complex. A maximum concentration of the dimer will be present at pH = pK_1. Since the dissociation of the dimer is the rate-determining step under such conditions, the observed reaction did not exhibit a meaningful sulfite concentration dependence. The subsequent reaction of the aqua complex with sulfite is significantly faster (see data for first step in temperature-jump experiments). An appropriate rate law for this process[44] is given in equation (15), which under the selected experimental

$$k_{obs} = \frac{4(k_{-10}K_1 + k_{-11}[H^+])}{K_1 + [H^+]} + k_{10} + k_{11}[H^+] \quad (15)$$

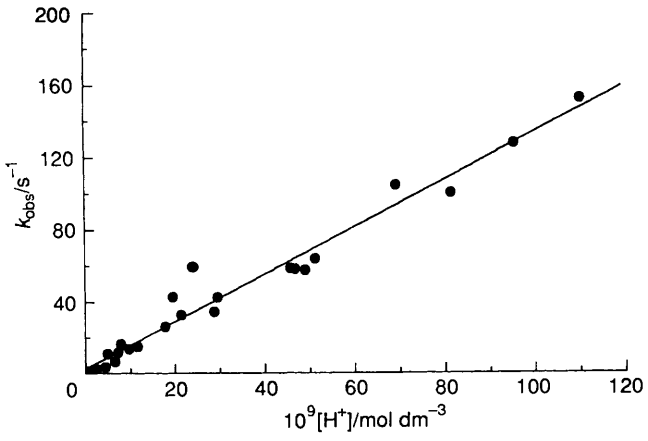

Fig. 10 Plot of k_{obs} *versus* $[H^+]$ for the data in Fig. 9(*b*) according to the reaction scheme (14)

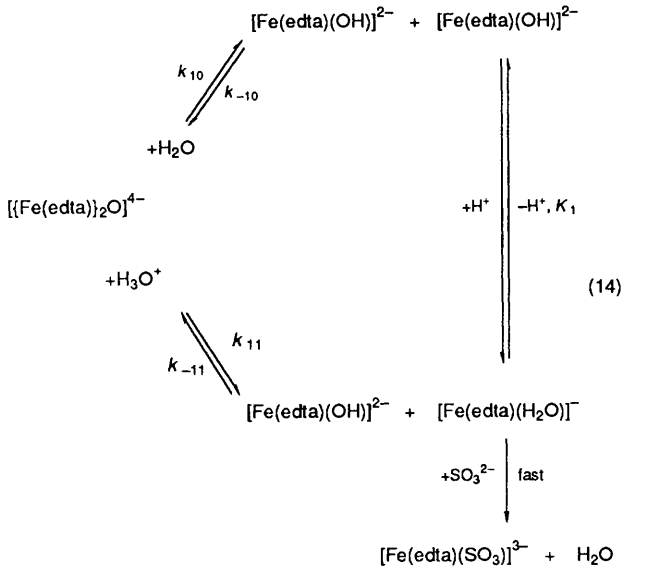

conditions simplifies to $k_{obs} = k_{10} + k_{11}[H^+]$.[44] The experimental data in Fig. 9(*b*) do exhibit a linear $[H^+]$ dependence, as shown in Fig. 10, with intercept 2.6 ± 2.3 s^{-1} (k_{10}) and slope (1.32 ± 0.05) × 10^9 dm^3 mol^{-1} s^{-1} (k_{11}). A similar plot for the data in Fig. 9(*a*) results in an intercept of 3.7 ± 1.9 s^{-1} and a slope of (1.10 ± 0.04) × 10^9 dm^3 mol^{-1} s^{-1}. The agreement between these two sets of data is remarkably good when the experimental error limits are taken into consideration, and demonstrates once again that the same kinetic step is observed in the absence and presence of sulfite under these experimental conditions. The kinetics of the spontaneous and acid-catalysed dissociation of the dimer (k_{10} and k_{11}, respectively) has been studied before.[44] The reported values are $k_{11} = 5 \times 10^8$ dm^3 mol^{-1} s^{-1} and $k_{10} = 1.2$ s^{-1} at 25 °C and 1.0 mol dm^{-3} ionic strength.[44] These values are close to those reported above. It follows that dissociation of the dimer is the rate-determining step under such conditions and can account for the slow reaction step observed in both the absence and presence of sulfite.

Conclusion

The results of this study have clearly indicated the ability of $[Fe(edta)]^-$ to produce a 1:1 S-bonded sulfito complex. Neither the equilibrium nor kinetic observations indicate the formation of a higher substituted complex, from which it follows that the *trans* labilization effect of co-ordinated sulfite is not capable of labilizing the edta ligand. The substitution process is controlled by the lability of the $[Fe(edta)(H_2O)]^-$ species and can only be observed kinetically on a temperature-jump time-scale. The pH dependence of the substitution reaction is related to the formation of inert hydroxo and oxo-bridged species. The $[Fe(edta)(H_2O)]^-$ complex exhibits dissociative behaviour and the limiting rate constant reached at high sulfite concentration is in close agreement with the solvent-exchange rate constant reported in the literature. This result demonstrates how the chelation effect induces the labilization of the co-ordinated water molecule and favours a seven-co-ordinate structure for the aqua complex. Kinetic processes observed on a millisecond time-scale are due to the rate-determining dissociation of an oxo-bridged dimeric species. Finally, the results reported in this study illustrate the difficulties encountered in kinetic studies on the substitution behaviour of metal edta complexes in general.

Acknowledgements

The authors gratefully acknowledge financial support from the Deutsche Forschungsgemeinschaft, Fonds der Chemischen Industrie, Bundesministerium für Forschung und Technologie, and the Commision of the European Communities (STEP Programme).

References

1 S. Rahal and H. W. Richter, *J. Am. Chem. Soc.*, 1988, **110**, 3126.
2 C. Bull, G. J. McClune and J. A. Fee, *J. Am. Chem. Soc.*, 1983, **105**, 5290.
3 S. Ahmad, J. D. McCallum, A. K. Shiemke, E. H. Appelman, T. M. Loehr and J. Sanders-Loehr, *Inorg. Chem.*, 1988, **27**, 2230.
4 K. C. Francis, D. Cummins and J. Oakes, *J. Chem. Soc., Dalton Trans.*, 1985, 493.
5 E. N. Rizkalla, O. H. El-Shafey and N. M. Guindy, *Inorg. Chim. Acta*, 1982, **57**, 199.
6 J. D. Rush and W. H. Koppenol, *J. Am. Chem. Soc.*, 1988, **110**, 4957.
7 R. P. Herzberg and P. B. Dervan, *Biochemistry*, 1984, **23**, 3934.
8 R. S. Youngquist and P. B. Dervan, *J. Am. Chem. Soc.*, 1985, **107**, 5528.
9 P. B. Dervan, *Science*, 1986, **232**, 464.
10 J. Kraft and R. van Eldik, *J. Chem. Soc., Chem. Commun.*, 1989, 790.
11 J. Kraft and R. van Eldik, *Inorg. Chem.*, 1989, **28**, 2297.
12 J. Kraft and R. van Eldik, *Inorg. Chem.*, 1989, **28**, 2306.
13 J. Kraft and R. van Eldik, *Atmos. Environ.*, 1989, **23**, 2709.
14 K. Bal Reddy, N. Coichev and R. van Eldik, *J. Chem. Soc., Chem. Commun.*, 1991, 481.
15 M. R. Hoffmann and J. G. Calvert, *Chemical Transformation Modules for Eulerian Acid Deposition Models*, vol. 2.
16 L. R. Martin and M. W. Hill, *Atmos. Environ.*, 1987, **21**, 1487.
17 T. E. Graedel, C. J. Weschler and M. L. Mandlich, *Nature (London)*, 1985, **317**, 240.
18 M. Dellert-Ritter and R. van Eldik, following paper.
19 J. Kraft, S. Wieland, U. Kraft and R. van Eldik, *GIT Fachz. Lab.*, 1987, **31**, 560.
20 H. Ogino and M. Shimura, *Adv. Inorg. Bioinorg. Mechn.*, 1986, **4**, 107.
21 J. K. Hovey and P. R. Tremaine, *J. Phys. Chem.*, 1985, **89**, 5541.
22 J. L. Hoard, M. Lind and J. V. Silverton, *J. Am. Chem. Soc.*, 1961, **83**, 2770.
23 M. D. Lind, J. L. Hoard, M. J. Hamor and T. A. Hamor, *Inorg. Chem.*, 1964, **3**, 34.
24 J. M. Lopez-Alcala, M. C. Puerta-Vizcaino, F. Conzalez-Vilchez, E. N. Duelser and R. E. Tapscott, *Acta Crystallogr., Sect. C*, 1984, **40**, 939.
25 X. Solans, M. F. Altabe, and J. Carcia-Oricain, *Acta Crystallogr., Sect. C*, 1984, **40**, 635.
26 J. F. Whidby and D. E. Leyden, *Anal. Chim. Acta*, 1970, **51**, 25.
27 C. Manley, *Z. Angew. Phys.*, 1971, **32**, 187.
28 J. Bloch and G. Navon, *J. Inorg. Nucl. Chem.*, 1980, **42**, 693.
29 J. Oakes and E. G. Smith, *J. Chem. Soc., Faraday Trans. 1*, 1983, 543.
30 K. C. Francis, D. Cummins and J. Oakes, *J. Chem. Soc., Dalton Trans.*, 1985, 493.
31 C. Bull, G. J. McClune and J. A. Fee, *J. Am. Chem. Soc.*, 1983, **105**, 5290.
32 K. Kanamori, H. Dohniwa, N. Ukita, I. Kanesaka and K. Kawai, *Bull. Chem. Soc. Jpn.*, 1990, **63**, 1447.
33 T. Mizuta, T. Yamamoto, K. Miyoshi and Y. Kushi, *Inorg. Chim. Acta*, 1990, **175**, 121.

34 C. H. L. Kennard, *Inorg. Chim. Acta*, 1967, **1**, 347.
35 S. A. Cotton, *Chem. Phys. Lett.*, 1976, **41**, 606.
36 L. E. Gerdom, N. A. Baenziger and H. M. Goff, *Inorg. Chem.*, 1981, **20**, 1606.
37 Y. Kushi, K. Morimasa, and H. Yoneda, 49th Annual Meeting Chemical Society of Japan, Tokyo, 1984, IN 31.
38 W. D. Wheeler and J. I. Legg, *Inorg. Chem.*, 1984, **23**, 3798.
39 K. Kanamori and K. Kawai, *Inorg. Chem.*, 1986, **25**, 3711.
40 G. Schwarzenbach and J. Heller, *Helv. Chim. Acta*, 1951, **34**, 576.
41 H. J. Schugar, A. T. Hubbard, F. C. Anson and H. B. Gray, *J. Am. Chem. Soc.*, 1969, **91**, 71.
42 R. L. Gustafson and A. E. Martell, *J. Phys. Chem.*, 1963, **67**, 576.
43 A. Marton, N. Sükösd-Roslosnik, A. Vertes, I. Nagy-Czako and K. Burger, *Inorg. Chim. Acta*, 1987, **137**, 173.
44 R. G. Wilkins and R. E. Yelin, *Inorg. Chem.*, 1969, **8**, 1470.
45 G. McLendon, R. J. Motekaitis and A. E. Martell, *Inorg. Chem.*, 1976, **15**, 2306.
46 D. T. Sawyer and J. M. McKinnie, *J. Am. Chem. Soc.*, 1960, **82**, 4191.
47 K. Nakamoto, *Infrared and Raman Spectra of Inorganic and Coordination Compounds*, 4th edn., Wiley, New York, 1986, p. 258.
48 M. Dellert-Ritter, Doctoral thesis, University of Witten/Herdecke, Witten, 1991.
49 M. Mizuno, S. Funahashi, N. Nakasuka and M. Tanaka, *Inorg. Chem.*, 1991, **30**, 1550.
50 H. Sakane, I. Watanabe, K. Ono, S. Ikeda, S. Kaizaki and Y. Kushi, *Inorg. Chim. Acta*, 1990, **178**, 67.

Received 17*th September* 1991; *Paper* 1/04814G